ELSEVIER

Earth and Planetary Science Letters 203 (2002) 329–341

EPSL

www.elsevier.com/locate/epsl

Ordovician palaeogeography with new palaeomagnetic data from the Montagne Noire (Southern France)

E. Nysæther [a,b], T.H. Torsvik [c,d,e,*], R. Feist [f], H.J. Walderhaug [b], E.A. Eide [g]

[a] *Norsk Hydro, Sandsliveien 90, 5049 Sandsli, Norway*
[b] *Institute of Solid Earth Physics, Allegatan 41, 5007 Bergen, Norway*
[c] *VISTA, c/o Geodynamics Centre, NGU, Leiv Eirikssons vei 39, 7491 Trondheim, Norway*
[d] *Institute of Petroleum Technology and Applied Geophysics, NTNU, 7494 Trondheim, Norway*
[e] *Department of Geology, Lund University, Sölvegatan 13, 223 62 Lund, Sweden*
[f] *Institut des Sciences de l'Evolution, Laboratoire de Paléobotanique et Paléontologie, Université Montpellier II, Place E. Bataillon, Cc 062, 34095 Montpellier Cedex 05, France*
[g] *Geodynamics Centre, NGU, Leiv Eirikssons vei 39, 7491 Trondheim, Norway*

Received 1 April 2002; received in revised form 5 July 2002; accepted 10 July 2002

Abstract

A joint palaeomagnetic and $^{40}Ar/^{39}Ar$ study has been performed on two olistolithic blocks from the Cabrières Wildflysch in the Montagne Noire region of the Massif Central in France. There, andesitic volcanic and volcaniclastic rocks of Llanvirn–Early Caradoc age (ca 470–458 Ma) occur. Despite extensive secondary alteration, destruction of the dominant magnetic mineral phase and $^{40}Ar/^{39}Ar$ whole rock experiments that demonstrate that the volcanic rocks suffered significant argon loss, a positive fold test and the presence of dual polarities suggest that a primary, Ordovician magnetisation has mostly survived. This is one of the few documented cases where the argon system was substantially reset whilst a subordinate set of small, relatively unaltered magnetite grains, probably hosted in silicates, still carry the original, in this case Ordovician, remanence.

The new data show that the Montagne Noire region was located at high southerly latitudes ($68° {}^{+17}/_{-15}$) during the Mid-Ordovician. This latitude represents the location for NW Gondwana of which the Massif Central was a part. Palaeomagnetic data from all the Central European massifs and terranes demonstrate a close link to the Gondwana Margin during the Lower and Middle Ordovician.

Keywords: paleomagnetism; Central Massif; Armorican Massif; Ordovician; paleogeography

1. Introduction

Reliable palaeomagnetic data and related poles from Northern Gondwana elements have been notoriously difficult to extract due to the multiple metamorphic and deformational events witnessed by the rocks; these difficulties apply especially to the earlier Palaeozoic units, which have had the least preservation potential. The Montagne Noire is located in the southernmost part of the French Massif Central (Fig. 1a,b) as part of the 'external

* Corresponding author. Tel.: +47-73-904000; Fax: +47-73-921620.
E-mail address: trond.torsvik@ngu.no (T.H. Torsvik).

0012-821X/02/$ – see front matter © 2002 Elsevier Science B.V. All rights reserved.
PII: S0012-821X(02)00847-6

zone', or Southern Palaeozoic Nappe Complex, and comprises a metamorphic dome of Late Proterozoic–Cambrian gneisses and schists embraced by low-grade palaeozoic sediments [1–3]. Montagne Noire formed part of NW Gondwana in the Lower Palaeozoic. The external zone of the Massif Central was only weakly metamorphosed during the protracted phase of Variscan tectonics that otherwise affected medium- to high-grade metamorphism of various crystalline units of the 'internal zones' of the region [4]. The Massif Central contains numerous, juxtaposed Northern Gondwanan crustal fragments amalgamated throughout Late Palaeozoic time to the southern margin of the Laurussian continent. Accretion of these elements to Laurussia preceded collision of the Gondwana continent with the Laurussian landmass as the Rheic Ocean finally closed.

Because of the problems of preservation in the internal zones, the rocks of the external zone of the Massif Central are attractive candidates for palaeomagnetic analysis. The allochthonous nappes surrounding the crystalline metamorphic domes comprise weakly to non-metamorphosed sedimentary and volcanic rocks ranging from Cambrian through Carboniferous ages with well-characterised stratigraphic and structural controls. We conducted a palaeomagnetic and $^{40}Ar/^{39}Ar$ study on rocks in one section of these external zones – the southeasternmost Montagne Noire – to attempt to place better constraints on Ordovician palaeogeography of these Northern Gondwana units.

2. Regional geology and sampling

The Montagne Noire is divided into the Axial Zone (Proterozoic to early Palaeozoic gneiss domes and Late Carboniferous granites), a northern zone (a series of early Palaeozoic, low-grade allochthonous units), and a southern zone formed by stacked and southward verging recumbent sheets [5]. This southern zone constitutes an almost complete section of mainly shallow-water, very low-grade (low greenschist facies) to non-deformed, Early Cambrian to Early Carboniferous sediments. Late Viséan, synorogenic Variscan sedimentation is now exposed in the southeasternmost Cabrières area ('Ecailles de Cabrières' auct.); the Cabrières area is characterised by wild-flysch deposits with exotic blocks of various post-Cambrian ages emplaced by gravity slides [6]. Among these olistolithic masses are blocks comprising a nearly complete Ordovician succession, in great contrast to the lower nappe sequences further to the southwest, where only Trema-

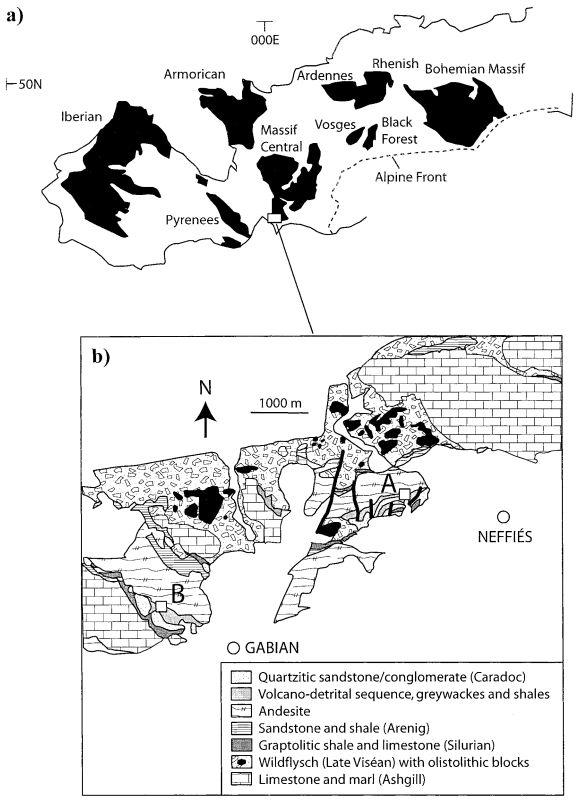

Fig. 1. (a) Sketch map showing the approximate outline of Variscan massifs [30]. (b) Location of sample sites from Block A at 2 km W of Neffiès village and from Block B at 1.6 km WNW of Gabian village, 'Ecailles de Cabrières' area, southeastern Montagne Noire. Samples from Block A have been taken on the northeastern foothill of Grand Glauzy Hill, 2 km E of Neffiès village along a road cut on the departmental road D125 from Roujan to Vailhan, 200 m N of the bridge crossing the Peyne river. Samples from Block B come from a road cut on road D13, 1.5 km W of Gabian and from a truck road immediately S of the tunnel below the abandoned railway, 200 m ENE of La Grange du Pin farmhouse.

doc and Early Arenig deposits are generally preserved.

In the Cabrières Zone, the Early Ordovician comprises several hundreds of meters of siliciclastic rocks with alternating sericitic shales and sandstones (Fig. 1b). Quartzitic concretions exhibiting cone-in-cone structures yield important trilobite faunas of Early Arenig age [7]. Lower Ordovician sediments are apparently conformably overlain by up to 150 m of andesitic volcanic and volcaniclastic rocks [8]. These comprise, from base to top: pyroclastic breccias, tuffs with intercalated rhyolitic effusives, greenish-blue chloritised microlithic porphyritic rocks and a sequence of volcano-detrital deposits containing breccias with volcanic debris, greywackes, shales and sandstones. Shaly interbeds at the top of the sequence yield poorly preserved acritarch remains among which F. Martin (written communication, 1976) recognised *Priscogalea striatula* and *Striatotheca principalis parva* of probably Mid-Ordovician, pre-Caradoc age. The volcaniclastic rocks are conformably overlain by conglomerates and quartzitic sandstones with benthic faunas including brachiopods, trilobites and cystoids. The brachiopods described by Havlicek [9] are of Mid- to Late Caradoc age.

The andesitic volcanic and volcaniclastic rocks of Mid- to possibly Early–Late Ordovician age (Llanvirn–Caradoc) are the focus of the present study, and 14 sites from two olistolithic blocks (Fig. 1b and Table 1) were sampled for palaeomagnetic analysis: six sites from one block (Block A) and eight sites from a more westerly block (Block B). Four of the Block B sites (sites 11–14) comprise volcaniclastic rocks, while the remaining sites are andesitic volcanic rocks. Two samples from these latter sites were also designated for $^{40}Ar/^{39}Ar$ analysis.

3. $^{40}Ar/^{39}Ar$ geochronology

Whole rock andesite samples F8 (site 1) and F92 (site 9) were crushed to 250 μm size prior to hand-picking and washing in distilled water and alcohol. Clean samples were packed in Sn-foil and irradiated at the Siloée reactor, Grenoble, France, and analysed in the $^{40}Ar/^{39}Ar$ laboratory at Université Blaise Pascal–CNRS, Clermont-Ferrand. Gas was released from the samples by incremental heating in a resistance furnace. The analytical procedure otherwise followed procedures outlined in Eide et al. [10].

Both release spectra yielded similar, very dis-

Table 1
Site mean statistics

Site	Rock	Block	J_{NRM}	n	N	Dec°	Inc°	k	α_{95}	BDec°	BInc°
1 (Ar)	AV	A	633 ± 8	12	12	81	−78	30	8	320	−61
2	AV	A	2.0 ± 1.4	11	11	117	−59	21	10	334	−82
3	AV	A	139 ± 17	9	9	137	−56	97	5	238	−82
4	AV	A	3.6 ± 1.8	13	14	110	−51	19	10	42	−81
5	AV	A	14.1 ± 4.7	7	8	109	−62	110	6	340	−78
6	AV	A	1.6 ± 0.2	3	4	94	−68	135	11	336	−69
7*	AV	B	38 ± 11	11	11	95	−55	79	5	82	−37
8*	AV	B	61 ± 7	10	10	187	−4	24	10	184	−19
9* (Ar)	AV	B	7.0 ± 2.4	10	11	252	10	30	9	252	−11
10	AV	B	144 ± 3	3	3	266	−66	613	5	330	−77
11	VC	B	38 ± 11	0	9	–	–	–	–	–	–
12	VC	B	6 ± 12	0	11	–	–	–	–	–	–
13	VC	B	3.7 ± 0.7	4	4	251	84	11	30	238	62
14	VC	B	2.1 ± 0.5	4	5	15	66	79	10	313	75

Block indicates sites from olistolitic Blocks A and B, respectively Fig. 1b); VC = volcaniclastic; AV = andesitic volcanics; J_{NRM} = mean NR intensities (10^{-3} A/m) with standard deviations; n = number of sample to calculate site means; N = total number of demagnetised samples; Dec°/Inc° = mean declination/inclination (in situ); k = Fisher precision parameter α_{95} = radius of 95% confidence circle BDec°/BInc° = bedding-corrected mean declination/inclination. No means were calculated from sites 11 and 12 owing to poorly defined components. The three sites marked with an asterisk were not used for calculating overall mean directions (Table 2). Ar = $^{40}Ar/^{39}Ar$ whole-rock experiment (Fig. 2).

turbed patterns with a group of three high gas-volume, low-temperature steps comprising ca 85% of the gas released in the experiments and yielding simple mean ages between ca 330 and 345 Ma (Fig. 2). The remainder of the gas, constituting the highest experimental temperatures, yielded steps with very variable apparent ages and high Cl/K ratios. The data from either sample, plotted on an inverse isochron, do not yield any sensible array through which to fit a line.

In a thin section, the dominant, relict igneous mineral in these samples is feldspar. However, pervasive growth of the secondary minerals chlorite, calcite, sericite on feldspar, and pseudomorphs of chlorite after what was perhaps amphibole, indicates an extensive, low-temperature, fluid-related overprint of these rocks under low greenschist-facies conditions. Low-grade metamorphism recrystallised the original, Ordovician igneous mineral assemblage and variably reset the argon isotopic content, apparently at the outcrop scale. The reset, whole-rock apparent ages fall within 330–345 Ma, or about the time of local granitic intrusions, significant deformation in the area and deposition of the wild flysch [1,2]. While tempting to link the apparent ages to events of similar age in the region, we do not attach any geologic significance to the $^{40}Ar/^{39}Ar$ data from these olistoliths due to their poor quality and inability to resolve the data on an inverse isochron.

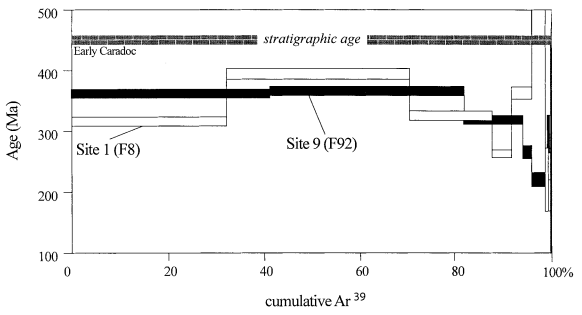

Fig. 2. ^{40}Ar–^{39}Ar whole-rock spectra for samples F8 (site 1) and F92 (site 9) that show apparent age as a function of the cumulative fraction of ^{39}Ar released. Height of boxes indicates analytical error ($\pm 1\sigma$) about each step. We do not attach geologic significance to the $^{40}Ar/^{39}Ar$ data.

4. Palaeomagnetic experiments

The natural remanent magnetisation (NRM) was measured using superconducting and spinner magnetometers, and the stability of NRM was tested with both thermal (MMTD60 furnace) and alternating field (two-axis tumbler) demagnetisation. Due to the presence of high-coercivity fractions in the volcaniclastic rocks and some andesite samples (not demagnetised in the maximum available field of 90 mT), thermal demagnetisation was employed for the bulk of the samples. Four andesitic sites have NRM intensities below 10^{-2} A/m. This is unusually low for volcanic rocks and attests to the almost total destruction of the dominant magnetic phase.

Typical examples of thermal demagnetisation behaviour (in situ) are given in Fig. 3. In general, the remanence quality is excellent for all Block A sites, but more variable in Block B.

Most andesites have well defined, steep, upward-pointing components (Fig. 3a,b), which show discrete unblocking near 580°C (Fig. 3f), suggesting magnetite as the principal remanence carrier. The same component continues into the haematite unblocking range in some specimens (Fig. 3a). Low-stability secondary magnetisations are present in some samples, but do not reveal any coherent directional pattern.

Remanence in the volcaniclastic rocks (Fig. 3c,d) is more complicated and curved demagnetisation paths suggest interplay of several overlapping components in most samples. Sites 11 and 12 have large low-stability components (Fig. 3c) residing in goethite (see later). These yield directions close to the present-day field, but components are difficult to identify in the higher blocking temperature ranges. Therefore, no mean directions have been calculated from these two sites. The remaining volcaniclastic sites (13 and 14) have downward-pointing magnetisations within the magnetite unblocking range (Fig. 3d) and yield roughly antipodal directions to the andesites.

Two andesitic sites from Block B (8 and 9) have anomalous shallow directions (Fig. 3e). Shallow inclinations accord with what should be expected from a Permo–Carboniferous or Hercynian overprint (e.g. [11,12]), although we do not have a

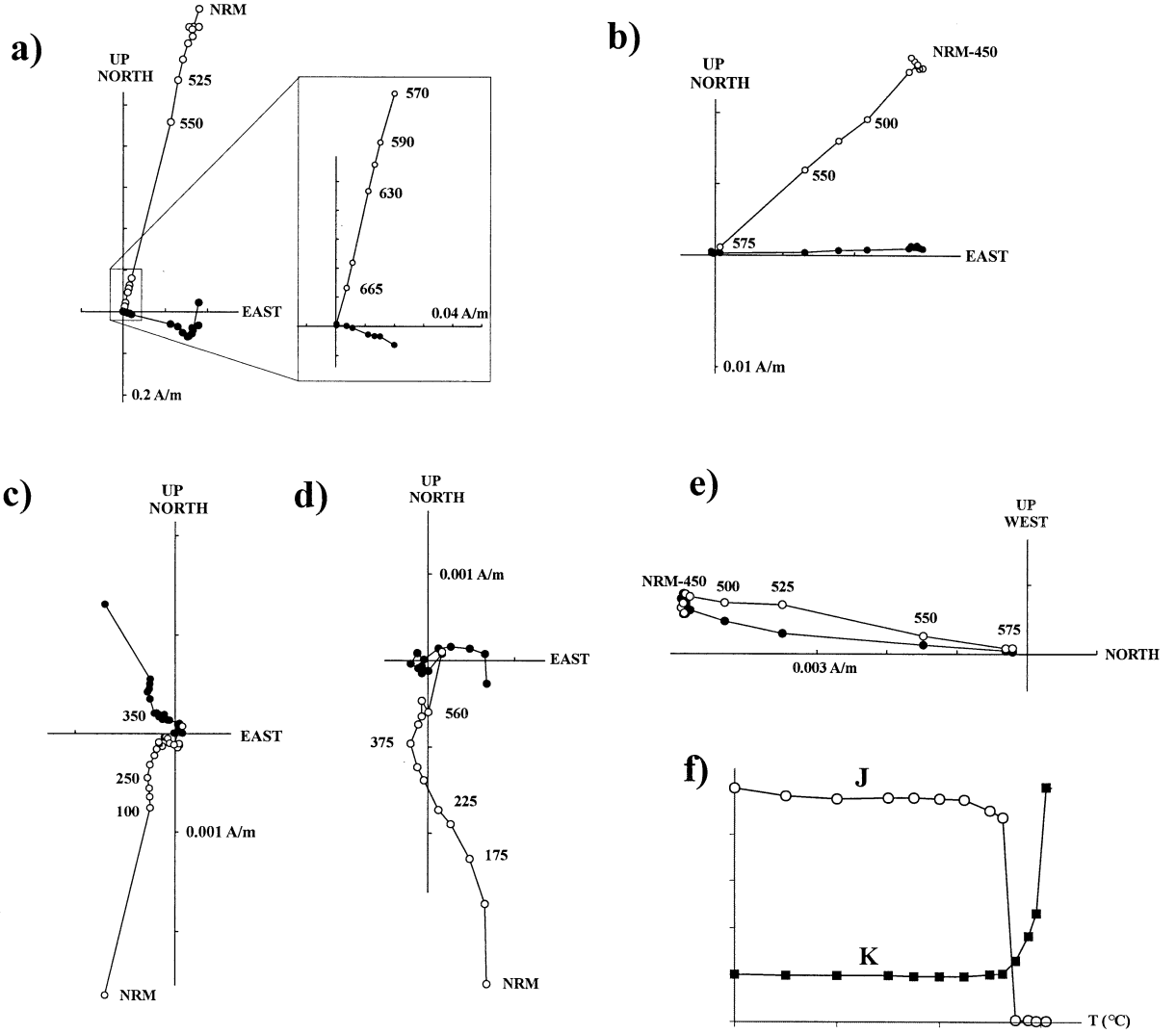

Fig. 3. Examples of thermal demagnetisation behaviour shown in orthogonal vector plots (in situ co-ordinates). Open (solid) symbols represent projections onto the vertical (horizontal) planes respectively. (a) Block A (site 1) andesite specimen showing a single, well defined component carried by magnetite and hematite. Inset shows an enlargement of the final demagnetisation steps. (b) Block B (site 7) andesite containing magnetite only. (c,d) Block B volcaniclastic (from sites 11 and 13, respectively), illustrating complex demagnetisation behaviour. The large initial intensity drop in (c) is attributed to the presence of goethite. (e) Example of anomalous shallow directions encountered in andesites at site 9. (f) Typical intensity decay spectra (J) and susceptibility change during demagnetisation (K) for the andesites.

viable explanation why these particular sites should have been preferentially remagnetised or developed their large declination difference.

A summary of site mean directions is given in Fig. 4a. Removal of the two shallow sites (8 and 9) before final analysis is unproblematic and compared with reference inclinations for Laurussia [13], site 8 and 9 inclinations clearly indicate a Permo–Carboniferous age. We have also elected to remove a third andesitic site from Block B (site 7, Fig. 4a), where specimens have slightly anomalous directions combined with low coercivity and a weathered appearance at outcrop. This leaves six Block A and three Block B sites for the final

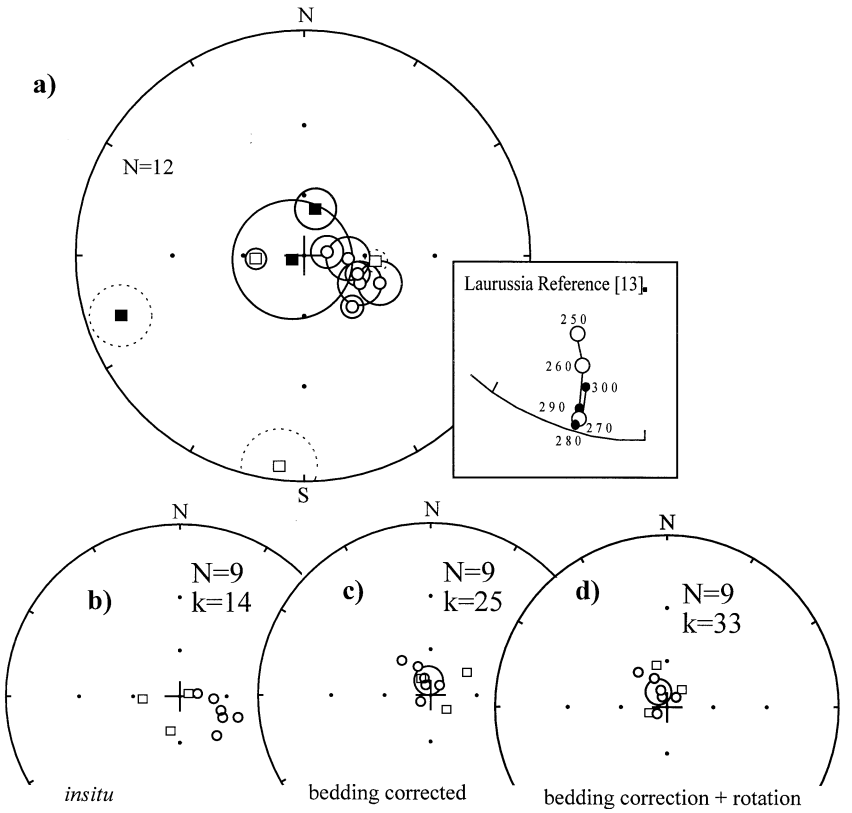

Fig. 4. Site mean directions and α_{95} confidence circles. Open (closed) symbols denote up-pointing (down-pointing) directions. Circular (squared) symbols denote sites from Block A (Block B). N = total number of plotted sites. K = Fisher precision parameter. (a) All calculated site means. Sites with stippled α_{95} circles were not used in the analysis. Inset stereoplot shows Laurussia Permo–Carboniferous reference directions recalculated from [13] to our sampling sites (ca 44°N, 3.5°E). (b) Site means from the nine sites used before tectonic correction. (c) Site means after correcting for tectonic tilt of the two blocks. (d) Site means after tilt correction and a 91° counter-clockwise rotation about a vertical axis for Block B (see text).

analysis. These are shown in Fig. 4b (in situ coordinates) after inverting the two downward-dipping volcaniclastic sites. Rotating both blocks back to the palaeo-horizontal (employing bedding information from stratigraphically overlying sediments (Block A) and volcaniclastic rocks (Block B)) results in a marked improvement in precision (Fig. 4c). The reduction in spread just fails to be significant at the 95% confidence level using the classical fold test of McElhinny [14], but the data pass the more modern test developed by McFadden and Jones [15]. It is further possible to improve the remanence grouping by invoking relative rotations of the two blocks around vertical

Table 2
Mean values calculated for Block A separately and for the combined results

	N (sites)	Mean inclination	Paleolatitude
Block A	6	-78.4 ± 10.4	$-68\ ^{+17}_{/-20}$
A+B combined	9	-81.3 ± 10.5	$-73\ ^{+19}_{/-17}$
A+B rotated	9	-78.4 ± 9.1	$-68\ ^{+15}_{/-17}$

All sites are bedding-corrected. Inclination and palaeolatitude are given with 95% confidence limits. See text for further explanation.

axes during flysch formation. Such rotations are highly probable, but unfortunately only the palaeo-horizontal can be determined from geological indices. Relative rotations around a vertical axis may, however, be determined by comparing declination differences between the two blocks. Rotating Block B 91° counter-clockwise, to make the mean declinations of the two blocks coincide (Fig. 4d), gives a further small increase in precision, but it should be noted that the steepness of the directions makes this declination correction somewhat arbitrary.

The uncertainty related to rotations around vertical axes implies that a formal reversal test [16,17] on the data is not straightforward since only inclinations of normal and reverse sites from different blocks may be compared with confidence. At site level, the two normal polarity sites from Block B yield a mean inclination of 72°

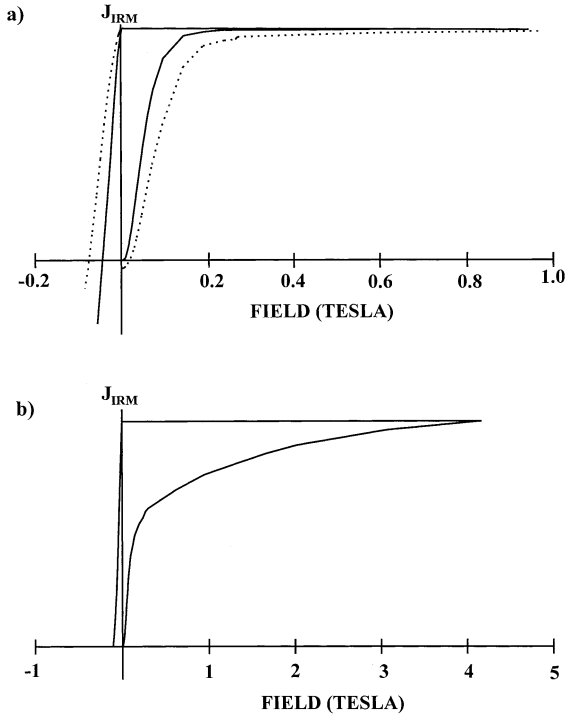

Fig. 5. Representative IRM acquisition and backfield curves. (a) Two andesitic specimens indicating, respectively, magnetite only (continuous line) and magnetite with minor haematite (stippled line). (b) volcaniclastic specimen with very high-coercivity mineral, presumably goethite. Note different scales on the horizontal axes.

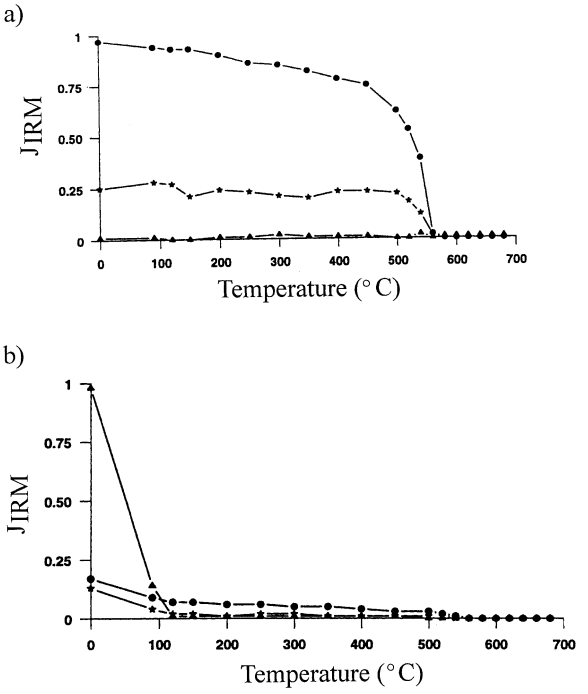

Fig. 6. Demagnetisation of three-axis IRM. Circles = low-coercivity fraction (0–0.1 T); Stars = intermediate-coercivity fraction (0.1–0.3 T); Triangles = high-coercivity fraction (0.3–4.2 T). (a) Andesitic specimen showing discrete magnetite blocking temperatures in the low and intermediate-coercivity fractions, and no remanence in the high-coercivity range. (b) volcaniclastic specimen with dominant goethite in the high-coercivity fraction and subordinate magnetite in the two lower-coercivity fractions.

whilst the seven reversed sites (six from Block A and one from Block B) yield a mean inclination of −78°, suggesting antipodal magnetisations within the error limits. Comparing normal and reverse data from Block B alone at specimen level, the means are not different at the 95% confidence level [16,18]. However, the more modern reversal test of McFadden and McElhinny [17] classifies the Block B test as 'indeterminate' (i.e. $\gamma_c > 20°$).

Mean inclinations and palaeolatitudes for the two options discussed above are given in Table 2, as well as values based on use of the (bedding-corrected) six sites from Block A alone. All three methods give consistent palaeolatitudes, but we favour the 'rotated' palaeolatitude of 68° which is identical to the value obtained from

Block A. Substituting the alternative 'unrotated' value of 73° does not greatly change the overall picture. We stress, however, that there is no way of knowing the absolute rotations in the flysch, so a pole position should not and cannot be calculated from our data.

The presence of both polarities and improved grouping after palaeo-horizontal corrections points towards a primary magnetisation. This is further supported by the steep remanence inclinations (incompatible with Hercynian directions), and indeed, these steep inclinations compare with those observed from many Central European massifs. It is therefore appropriate later to discuss the palaeolatitude estimate in the context of Ordovician palaeogeography.

5. Rock magnetic considerations

As Permo–Carboniferous (Hercynian) remagnetisations are the norm in many rocks from Central–South Europe, various techniques were employed in an attempt to elucidate the origin of the stable remanence. These methods included analysis of thermomagnetic curves, coercivity spectrum analysis and demagnetisation of three-axis isothermal remanent magnetisation (IRM) (procedure as in [19]), optical and scanning electron microscopy, as well as energy-dispersive X-ray spectrometry (EDXS). We also measured the anisotropy of magnetic susceptibility in order to test for strain and potential remanence deflection, but all measured samples yield low anisotropy values ($<3.5\%$) and the results are not further elaborated.

IRM-H curves (Fig. 5a), together with demagnetisation of three-axis IRM (Fig. 6a), confirm that the andesites are dominated by magnetite, occasionally accompanied by a small haematite fraction (as also seen in Fig. 3a). volcaniclastic rocks show the presence of a very high-coercivity mineral, which fails to saturate in the maximum available field of 4.2 T (Fig. 5b). Demagnetisation of three-axis IRM (Fig. 6b) clearly identifies this mineral as goethite, co-existing with a small amount of magnetite. The two sites where the goethite content was highest (sites 11 and 12) are the two sites which failed to give consistent remanence directions (Table 1).

Reflected light microscopy (Fig. 7) on andesitic samples reveals the presence of two distinct phases:

1. The most abundant magnetic phase originally consisted of titanomagnetite grains, commonly 25–75 μm in size, with lamellae attesting to high temperature (deuteric) oxidation (Fig. 7a). These grains are now highly altered by secondary oxidation, in most cases leading to total replacement of the original mineralogy by non-opaque phases. Further evidence for ex-

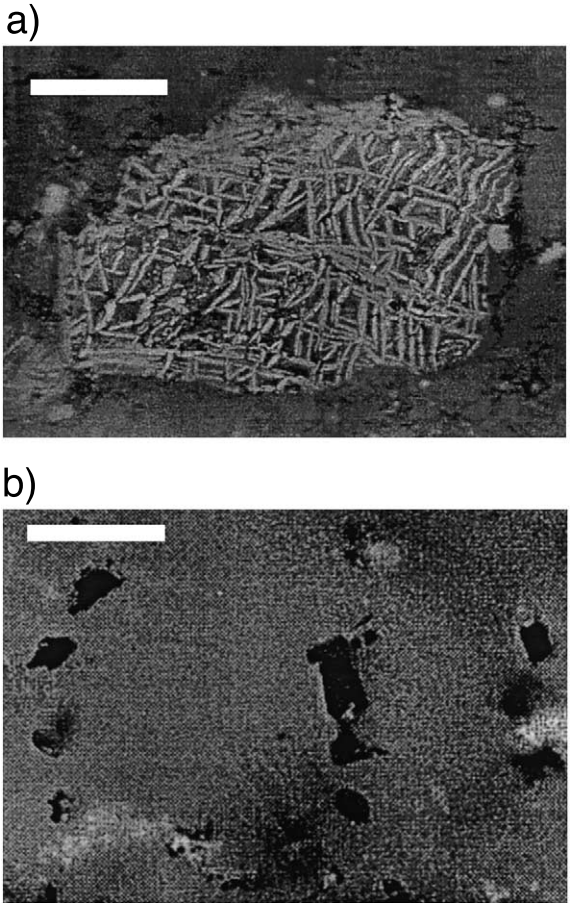

Fig. 7. Reflected light photomicrographs of opaque grains from andesites. Scale bars = 30 μm. (a) Titanomagnetite grain with extensive low-temperature alteration and replacement of original magnetite with non-opaque phases. (b) Subordinate smaller magnetite grains found as inclusions in silicates.

tensive alteration is given by EDXS, which shows that the lamellae consist of pure rutile whilst regions between lamellae have an iron content below 50%. This leads us to conclude that this phase is now, in effect, non-magnetic and does not contribute significantly to the remanence; this would also explain the very low NRM intensities encountered at most sites.

2. A separate opaque phase consisting of small (≤ 10 μm) cubic grains is present as inclusions in silicates (Fig. 7b). EDXS shows these to have a pure iron composition. We suggest this to be the origin of the magnetite and infer that a stable primary remanence has survived in this second phase. A well shielded microscopic location like an inclusion, together with a favourable macroscopic environment, e.g. protection from Hercynian deformation/fluids in large rigid olistolitic blocks, might explain the survival of a primary remanence in a region where Hercynian overprinting is regionally prevalent.

6. Palaeogeographic considerations

Because of gaps in the geological record and potential block rotations, robust APW paths are not available from individual European massifs, but Fig. 8a summarises the most reliable palaeolatitude estimates and compares them with predicted latitudes for the NW Gondwana Margin (recalculated to 45°N from the APW path of Torsvik and Van der Voo [20]). European massif latitudes should overlap (i.e. being Peri-Gondwanan as they all are in the Early–Mid Ordovician) or plot at lower latitudes. This is the case for all European massif latitudes, except one Late Ordovician estimate from the Armorican Massif (entry A5; see also Table 3).

In the Early Ordovician (480 ± 10 Ma), Avalonia (England–Wales), Armorica (see discussion on definition below) and Perunica (Bohemia) fringed the high-latitude areas of Gondwana (South America and Africa). The South Pole was located in Northern Africa, Laurentia was located at low-to-equatorial latitudes, whilst Baltica occupied intermediate to low southerly latitudes (Fig. 9a). Palaeomagnetic data and the characteristic Calymenacean–Dalmanitacean trilobite fauna from Gondwana/Peri-Gondwana clearly demonstrate oceanic separation from both Baltica and Laurentia (Fig. 9a). The strong linkage of the Montagne Noire, and the Cabrières area in particular, with Gondwana is clearly emphasised by affinity patterns of the trilobite faunas: out of 35 genera

Table 3
Compilation of inclinations (Inc.) and palaeolatitudes (P.Lat.) for European massifs and terranes

Formation, area	Code	Age range	Mean age	α_{95}	Inc.	P.Lat.	Reference
Pointe d'Armorique sediments, Brittany	A6	400–415	408	4.2	−35	−19	[31]
Catlan Ranges and Eastern Pyrenees	I2	414–418	416	8.5	−51	−32	[32]
Barrandian Basin volcanics–sediments, Perunica	P3	417–426	422	5.7	−40	−23	[33]
Thouars Massif, Armorican Massif	A5	444 ± 9[a]	444	7	−83	−76	[34]
Crozon Dolerites, Armorican Massif	A4	443–458	450	8	−63	−45	[35]
Barrandian Basin sediments–volcanics, Perunica	P2	443–458	451	9.5	−59	−40	[36]
Cabo de Penas, Iberia	I1	443–480	460	6	−78	−68	[37]
Montagne Noire, Massif Central	M	459–470	464	8.5	−78	−68	This study
Barrendian Basin volcanics–sediments, Perunica	P1	467–475	470	14.6	−83	−76	[33]
Pont-Rean Formation, Brittany	A3	470–485	478	6.5	−75	−62	[38]
Moulin de Chateaupanne Formation	A2	470–485	478	6	−81	−72	[35]
Saxothuringian Basin	S	478 ± 2[b]	478	11.6	−76	−64	[39]
Cap de la Chevre Formation, Brittany	A1	477–495	486	11	−71	−55	[40]

Age range (in Ma) is based on stratigraphic correlation unless otherwise noted. Code is used to identify the table entries in Fig. 8a.

[a] = Rb–SR.

[b] = U/Pb.

reported from this region, 79.4% occur in Gondwana, of which 45.7% are exclusively restricted to Gondwana [7].

Avalonia rifted off Gondwana in the Arenig–Llanvirn and drifted northward between 480 and 460 Ma (Fig. 9b), and the Ordovician transit across the closing Iapetus Ocean and the Tornquist Sea is seen by the changing affinities of Avalonian brachiopods from Gondwanan to a mixture of both Baltican and Laurentian affinities [21,22]. Before we continue our discussion, the definition of Armorica, defined in a modern sense by Van der Voo [23] to include most of Central Europe and Northern Africa, needs some clarification.

Matte [24] defined Armorica as a small but complex continental plate bordered to the north by the Rheic Ocean (Fig. 9b) and to the south by the Galicia–Southern Brittany (GSB; Fig. 9b) Ocean (see also [25]), and thus Armorica included only a small part of westernmost Iberia and Central Brittany and Normandy in France. Eastwards, Matte included the Saxothuringian and the Barrandian micro-plates as part of Armorica. Most of Iberia, Southern France (Massif Central and the Montagne Noire) and Corsica–Sardinia were part of Gondwana, since there are no known intervening Palaeozoic sutures.

On palaeomagnetic grounds, Torsvik and coworkers included the Armorican Massif and parts of the Iberian Massif within Armorica. Cocks and Torsvik [26] added the Massif Central and the Montagne Noire areas to Armorica (stippled outline in Fig. 9a), because intra-oceanic domains, if they existed, must have been small and undetectable on both faunal and palaeomagnetic grounds. Palaeomagnetic data from the Barrandian Basin of Perunica show high latitudes in the Early Ordovician (Figs. 8 and 9a), but intermediate latitudes recorded by the Late Ordovician have led to speculations that Perunica was a separate microblock. This is supported by faunal analysis [26]. Tait et al. [27], however, included Perunica in Armorica (defined as an assemblage of the Armorican and Iberian massifs, Perunica, Saxothuringian and the Catalan Terrane) and, based on Perunica data (see P1–3 in Fig. 8a), they argued that Armorica was separated from Gondwana by

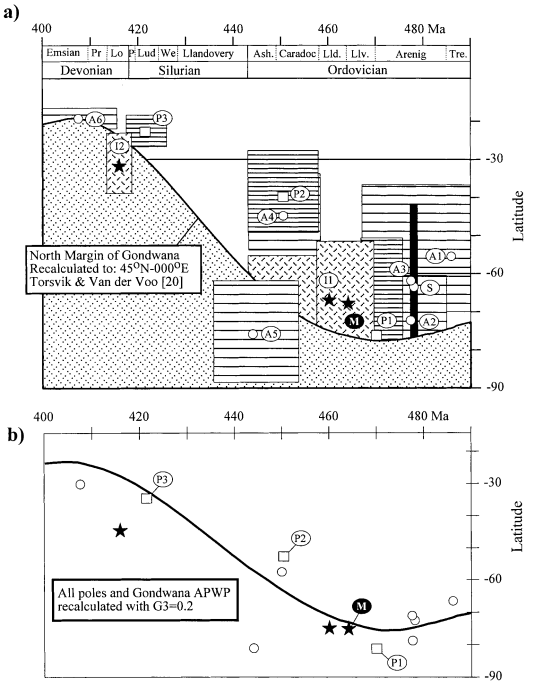

Fig. 8. (a) Compilation of palaeolatitudes derived from European massifs and terranes (Table 3). Boxes include uncertainty in both palaeolatitude (95% confidence level) and age. Codes A1–6 derived from the Armorican Massif, P1–3 from Perunica (Barrandian Basin), I1–2 from Iberia, S from Saxothuringian and M = this study (Montagne Noire, Massif Central). The expected position of the NW margin of Gondwana (which includes the Massif Central and most of Iberia) is calculated from [20]. (b) As in (a) but all palaeomagnetic data have been recalculated with G3 = 0.2 (octupole). Errors (see (a)) are not shown for purposes of diagram simplicity but essentially all European massifs and terranes will overlap with the Gondwana Margin within errors (see text).

a wide ocean in Late Ordovician and Silurian times.

In Fig. 9b we present a palaeogeographic reconstruction at ±460 Ma, where the Massif Central is approximately positioned according to our Cabrières data (68°S) and marks the NW Gondwana Margin along with parts of Iberia. Tait et al. [27] show a wide ocean (2000–4000 km) between Armorica and Gondwana from Late Ordovician (Ashgill) to Late Devonian times, but the width of that ocean (GSB, Fig. 9b) critically hinges on the position of Gondwana. Unfortunately, Gondwana is poorly constrained from

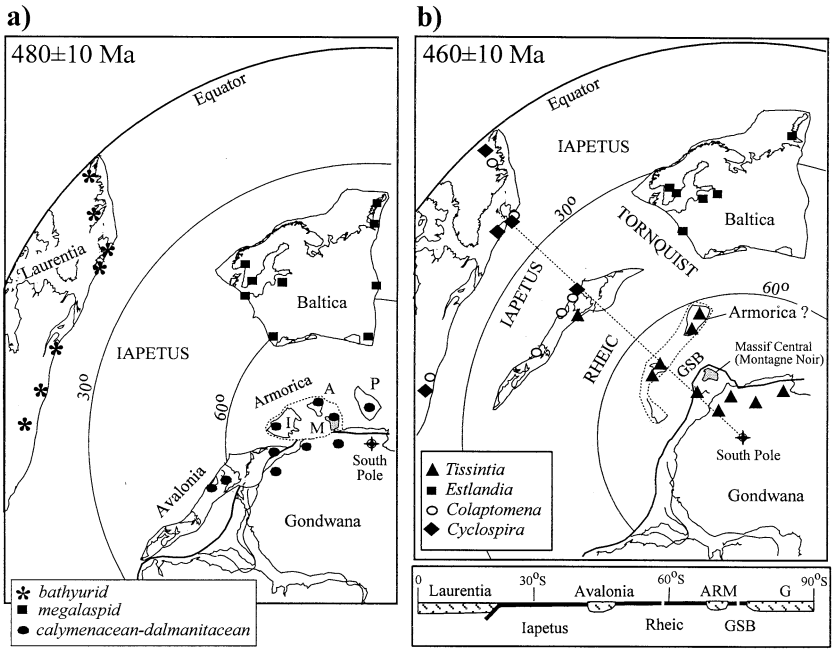

Fig. 9. (a) 480 ± 10 Ma reconstruction with some key Arenig–Llanvirn trilobite faunas from Gondwana/Peri-Gondwana, Baltica and Laurentia (after [26]). All faunal and palaeomagnetic data indicate close affinities with Northern Gondwana. I = Iberian Massif, A = Armorican Massif, M = Massif Central, P = Perunica. Equal-area polar projection. (b) 460 ± 10 Ma reconstruction with some key Caradoc brachiopod genera [26]. Massif Central is reconstructed in latitude based on the present study whilst NW Gondwana has been adjusted from [26] in order to maintain a close link between Gondwana and Massif Central. Armorica as defined by Matte [24] is shown with a possible but small oceanic separation from Massif Central/NW Gondwana (see text). GSB = Galicia–Southern Brittany Ocean. A schematic cross section from NW Gondwana to Laurentia is shown in the lower diagram. G = Gondwana, ARM = Armorica.

Mid-Ordovician to Devonian times (e.g. [20,26,28]) and by adopting a new APW path [20], oceanic separation between Armorica and Gondwana appears much narrower. Given the uncertainty in the palaeomagnetic data, GSB may only have been a few hundred kilometers wide at its maximum in Late Ordovician–Early Silurian times (Fig. 8a). Subduction beneath Armorica probably started in the Early Silurian and subsequently led to continental subduction and early Variscan (430–370 Ma) tectonism and metamorphism in the internal parts of the massif [24]. By the Devonian (Emsian), Armorica latitudes once again overlap with those of the Gondwana Margin (Fig. 8a).

We have so far discussed palaeomagnetic data on the assumption of a pure geocentric axial dipole (GAD) field. Van der Voo and Torsvik [29] expressed concerns about the validity of the GAD hypothesis and in a recent comparison of Gondwana and Laurussia APW paths, Torsvik and Van der Voo [20] argued for octupole (G3) contributions as high as 20% for parts of the Palaeozoic. If correct, this octupole contribution would result in very different Ordovician palaeogeographic scenarios, and we show the latitudinal consequences of a 20% octupole contribution in Fig. 8b. Palaeolatitude estimates for all the Central European massifs and terranes would be considerably higher (up to 15° of latitude) when corrected for G3 contributions, whilst the change for the Gondwana Margin is comparably smaller. Note that all European latitudes will overlap or will be very close to Gondwana Margin estimates (e.g. compare P1–P3 latitude in Fig. 8a,b); hence, any intervening ocean between Gondwana and Armorica will be much smaller and can essentially be eliminated by G3 fields in the order of 10–20%.

7. Conclusions

Despite extensive low-temperature secondary alteration, destruction of the dominant magnetic mineral phase and $^{40}Ar/^{39}Ar$ whole-rock experiments that indicate that the volcanic rocks suffered significant argon loss, a positive fold test and the presence of dual polarities demonstrate that a primary, Mid-Ordovician magnetisation has survived in the Cabrières Wildflysch. The reset, whole-rock apparent ages fall within 330–345 Ma, but we do not attach any geologic significance to the $^{40}Ar/^{39}Ar$ data due to their poor quality. These data, however, demonstrate that fluid and pressure–temperature conditions can function to reset the argon systematics of a rock or mineral assemblage, but may not affect the magnetic mineralogy carrying the remanent magnetisation. The primary Ordovician remanence is carried by magnetite grains as inclusions in silicates and, together with a favourable macroscopic environment such as protection from Hercynian deformation/fluids in large rigid olistolitic blocks, can explain the survival of a primary remanence in a region where Hercynian overprinting is regionally prevalent.

The palaeomagnetic data position the Montagne Noire region and the Massif Central at high southerly latitudes ($68° {}^{+17}/_{-15}$) during the Mid-Ordovician (Llanvirn–Early Caradoc). This is the first report of primary Ordovician latitudes from the Montagne Noire region, but the study area has probably undergone Variscan rotations and consequently a pole position should not be calculated. During the Palaeozoic, the Massif Central and the Montagne Noire were part of Gondwana and thus our palaeolatitude puts important constraints on the location of the NW margin of Gondwana during the Mid-Ordovician. Palaeomagnetic data from all the Central European massifs and terranes demonstrate a close link to the Gondwana Margin during the Lower and Middle Ordovician. By the Late Ordovician it is possible that parts of the Armorica assemblage had rifted off the NW Gondwana Margin (including Massif Central and most of Iberia), but the width of the intervening ocean was probably not very large.

Acknowledgements

We thank J.M. Lardeaux and L.R.M. Cocks for discussions, and P. Matte and an anonymous referee for valuable comments. NFR, the Geological Survey of Norway and VISTA are thanked for financial support. *[RV]*

References

[1] P. Ledru, A. Autran, D. Santallier, Lithostratigraphy of Variscan Terranes in the French Massif Central: A basis for palaeogeographical reconstruction, in: J.D. Keppie (Ed.), Pre-Mesozoic geology in France and Related areas, Springer, Heidelberg, 1994, pp. 276–288.

[2] P. Ledru, S. Costa, H.P. Echtler, Structure, in: J.D. Keppie (Ed.), Pre-Mesozoic geology in France and Related areas, Springer, Heidelberg, 1994, pp. 305–323.

[3] R. Feist, H. Echtler, J. Galtier, B. Mouthier, The Massif Central – Biostratigraphy and dynamics of the non-metamorphic sedimentary record, in: J.D. Keppie (Ed.), Pre-Mesozoic geology in France and related areas, Springer, Heidelberg, 1994, pp. 289–304.

[4] D.S. Santallier, J.M. Lardeaux, J. Marchand, Ch. Marignac, Metamorphism, in: J.D. Keppie (Ed.), Pre-Mesozoic Geology in France and Related Areas, Springer, Heidelberg, 1994, pp. 324–340.

[5] M. Demange, Contribution au problème de la formation des domes de la Zone axiale de la Montagne noire: analyse géométrique des plissements superposés dans les séries métasédimentaires de l'envelope. Implications poor tout modèle géodynamique, Géol. France 4 (1998) 3–56.

[6] W. Engel, R. Feist, W. Franke, Synorogenic gravitational transport in the Carboniferous of the Montagne Noire (S France), Z. dtsch. geol. Ges. 129 (1978) 461–472.

[7] P. Bérard, Trilobites de l'Ordovicien Inférieur des Monts de Cabrières, Mém. Centre d'Etudes et de Recherches géologiques et hydrologiques, Univ. Montpellier 24, 1986, pp. 1–220.

[8] H. Gonord, J.-P. Ragot, L. Saugy, Observations lithostratigraphiques nouvelles sur la série de base (Ordovicien inférieur) des nappes de Cabrières, region de Gabian-Glauzy (Montagne-Noire, Hérault), Bull. Soc. Géol. France 7 (1964) 419–427.

[9] V. Havlicek, Upper Ordovician brachiopods from the Montagne Noire, Palaeontographica A176 (1981) 1–34.

[10] E.A. Eide, T.H. Torsvik, T.B. Andersen, N.O. Arnaud, Early Carboniferous unroofing in western Norway: A tale of alkali feldspar thermochronology, J. Geol. 107 (1999) 353–374.

[11] V. Courtillot, P. Chambon, J.P. Brun, P. Rochette, A magnetotectonic study of the Hercynian Montagne Noire (France), Tectonics 5 (1986) 733–751.

[12] J.P. Cogne, J. Van den Driessche, J.P. Brun, Syn-exten-

sion rotations in the Permian St Affrique basin (Massif Central, France): palaeomagnetic constraints, Earth Planet. Sci. Lett. 115 (1993) 29–42.
[13] T.H. Torsvik, R. Van der Voo, J.G. Meert, J. Mosar, H.J. Walderhaug, Reconstructions of the continents around the North Atlantic at about the 60th parallel, Earth Planet. Sci. Lett. 187 (2001) 55–69.
[14] M.W. McElhinny, Statistical significance of the fold test in palaeomagnetism, Geophys. J. Astron. Soc. 8 (1964) 338–340.
[15] P.L. McFadden, D.L. Jones, The fold test in palaeomagnetism, Geophys. J. Astron. Soc. 67 (1981) 53–58.
[16] G.S. Watson, Analysis of dispersion on a sphere, Mon. Not. R. Astron. Soc. Geophys. Suppl. 7 (1956) 153–159.
[17] P.L. McFadden, M.W. McElhinny, Classification of the reversal test in palaeomagnetism, Geophys. J. Int. 103 (1990) 725–729.
[18] P.L. McFadden, F.J. Lowes, The discrimination of mean directions drawn from Fisher distributions, Geophys. J. R. Astron. Soc. 67 (1981) 19–33.
[19] W. Lowrie, Identification of ferrormagnetic minerals in a rock by coercivity and unblocking temperature properties, Geophys. Res. Lett. 17 (1990) 159–162.
[20] T.H. Torsvik, R. Van der Voo, Refining Gondwana and Pangea palaeogeography: Estimates of Phanerozoic non-dipole (octupole) fields, Geophys. J. Int., in press.
[21] L.R.M. Cocks, R.A. Fortey, Faunal evidence for oceanic separations in the Palaeozoic of Britain, J. Geol. Soc. Lond. 139 (1982) 465–478.
[22] T.H. Torsvik, A. Trench, The Ordovician history of the Iapetus Ocean in Britain: New palaeomagnetic constraints, J. Geol. Soc. Lond. 148 (1991) 423–425.
[23] R. Van der Voo, Paleozoic assembly of Pangea: a new plate tectonic model for the Taconic, Caledonian and Hercynian orogenesis (abstract), EOS Trans. AGU 60 (1979) 241.
[24] P. Matte, The Variscan collage and orogeny (480–290 Ma) and the tectonic definition of the Armorica microplate: a review, Terra Nova 13 (2001) 122–128.
[25] P. Rey, J.-P. Burg, M. Casey, The Scandinavian Caledonides and their relationship to the Variscan belt, in: J.-P. Burg, M. Ford (Eds.), Orogeny Through Time, Geol. Soc. Spec. Publ. 121, 1997, pp. 179–200.
[26] L.R.M. Cocks, T.H. Torsvik, Earth Geography from 500 to 400 million years ago: a faunal and palaeomagnetic review, J. Geol. Soc. Lond., in press.
[27] J. Tait, M. Schatz, V. Bachtadse, H. Soffel, Palaeomagnetism and Palaeozoic palaeogeography of Gondwana and European terranes, in: W. Franke, V. Haak, O. Oncken, D. Tanner (Eds.), Orogenic Processes: Quantification and Modelling in the Variscan Belt, Geol. Soc. Lond. Spec. Publ. 179, 2000, pp. 21–34.
[28] R. Van der Voo, Paleomagnetism of the Atlantic, Tethys and Iapetus Oceans, Cambridge University Press, Cambridge, 1993, 411 pp.
[29] R. Van der Voo, T.H. Torsvik, Evidence for Permian and Mesozoic non-dipole fields provides an explanation for the Pangea reconstruction problems, Earth Planet. Sci. Lett. 187 (2001) 71–81.
[30] W. Franke, Variscan plate tectonics in Central Europe – current ideas and open questions, Tectonophysics 169 (1989) 221–228.
[31] J. Tait, New Early Devonian paleomagnetic data from NW France: paleogeography and implications for the Armorican microplate hypothesis, J. Geophys. Res. 104 (1999) 2831–2839.
[32] J. Tait, V. Bachtadse, J. Dinarës-Turell, Paleomagnetism of Siluro-Devonian sequences, NE Spain, J. Geophys. Res. 105 (2000) 23595–23603.
[33] J. Tait, V. Bachtadse, H. Soffel, New palaeomagnetic constraints on the position of central Bohemia during Early Ordovician times, Geophys. J. Int. 116 (1994) 131–140.
[34] H. Perroud, R. Van der Voo, Palaeomagnetism of the late Ordovician Thouars Massif, Vendee Province, France, J. Geophys. Res. 90 (1985) 4611–4625.
[35] H. Perroud, N. Bonhommet, J.P. Thebault, Palaeomagnetism of the Ordovician Moulin de Chatteapanne Formation, Vendee, western France, Geophys. J. Astr. Soc. 85 (1986) 573–582.
[36] J. Tait, V. Bachtadse, H. Soffel, Upper Ordovician palaeogeography of the Bohemian Massif: implications for Armorica, Geophys. J. Int. 122 (1995) 211–218.
[37] H. Perroud, Palaeomagnetism of Palaeozoic rocks from the Cabo de Penas, Asturia, Spain, Geophys. J. Astr. Soc. 75 (1983) 201–215.
[38] J.P. Cogne, Strain magnetic fabric, and paleomagnetism of the deformed redbeds of the Pont-Rean Formation, Brittany, France, J. Geophys. Res. 93 (1988) 13673–13687.
[39] M. Schatz, T. Reischmann, J. Tait, V. Bachtadse, H. Bahlburg, U. Martin, The early Palaeozoic break-up of northern Gondwana, a case study from the Saxothuringian Basin, Eastern Variscan Fold Belt, Geophys. J., in press.
[40] J.P. Cogne, N. Bonhommet, V. Kropacek, T. Zelinka, E. Petrovski, Paleomagnetism and magnetic fabric of the deformed redbeds of the Cap de la Chevre formation, Brittany, France, Phys. Earth Planet. Int. 67 (1991) 374–388.